For submission to Chemical Communications as a communication

Challenging Conventional f-Element Separation Chemistry – Reversing Uranyl(VI)/Lanthanide(III) Solvent Extraction Selectivity

Supporting Information

Experimental Procedures.

General Methods. Acid and base solutions were standardized, and solution pH and pC_H (-log $[H^+]$) measured, by potentiometry using a semi-micro refillable electrode (Beckman-Coulter, Indianapolis, IN), which was calibrated by standard pH solutions (Fisher Scientific,) and by Gran titration.

Materials. All chemicals used in these procedures were certified reagent grade or higher and used without further purification, unless noted otherwise. Deionized water was obtained from a deionized feed such that the resistivity was at least 18 MΩ*cm^{-1}. For the solution spectroscopy and solvent extraction experiments a 0.010 M $UO_2(NO_3)_2$ working stock solution was prepared from a commercial ICP standard solution of depleted (0.2% ^{235}U) uranyl nitrate (1000 ppm, Inorganic Ventures, Christiansburg , VA, USA) by diluting with deionized water and adjusting the pH to 4.0 dropwise with a KOH solution. Synthesis of $Na_2[UO_2(salen\text{-}SO_3)(OH_2]\cdot 9H_2O$ was undertaken using available samples of depleted uranyl nitrate hexahydrate. Lanthanide nitrate stock solutions were prepared from their oxides (Michigan Metals & Manufacturing, Inc., West Bloomfield, MI, 99.99%) by dissolving in concentrated nitric acid. Excess nitric acid was removed by evaporating to near dryness and adding dilute nitric acid in several cycles. The final solutions were reconstituted to 0.1 M lanthanide ion with 1 x 10^{-3} M HNO_3 and the concentrations were verified by ion-exchange titration or ICP-MS. HDEHP (Di(2-ethylhexyl)phosphate, 95%, ACROS Organics, Geel, Belguim) was purified using the Cu(II) complexation method.[1] The synthesis of 5-sulfo-salicylaldehyde sodium salt and the desired ligand, N,N'-bis(salicylidene-5-sulfonato)-diaminoethane disodium salt, were adapted from previously published procedures synthesized and are described in Scheme 1.[2-4]

Synthesis and Characterization.

Synthesis of *N,N'*-bis(5-sulfonato- salicylidene)-diaminoethane disodium salt (H_2salen-SO_3)

The synthesis of H_2salen-SO_3 was carried out in accord with previously published procedures by the steps described in Scheme 1.[2-4]

Scheme 1. Synthesis of 5-sulfonato-salicylaldehyde sodium salt and N,N'-bis(salicylidene-5-sulfonato)-diaminoethane disodium salt

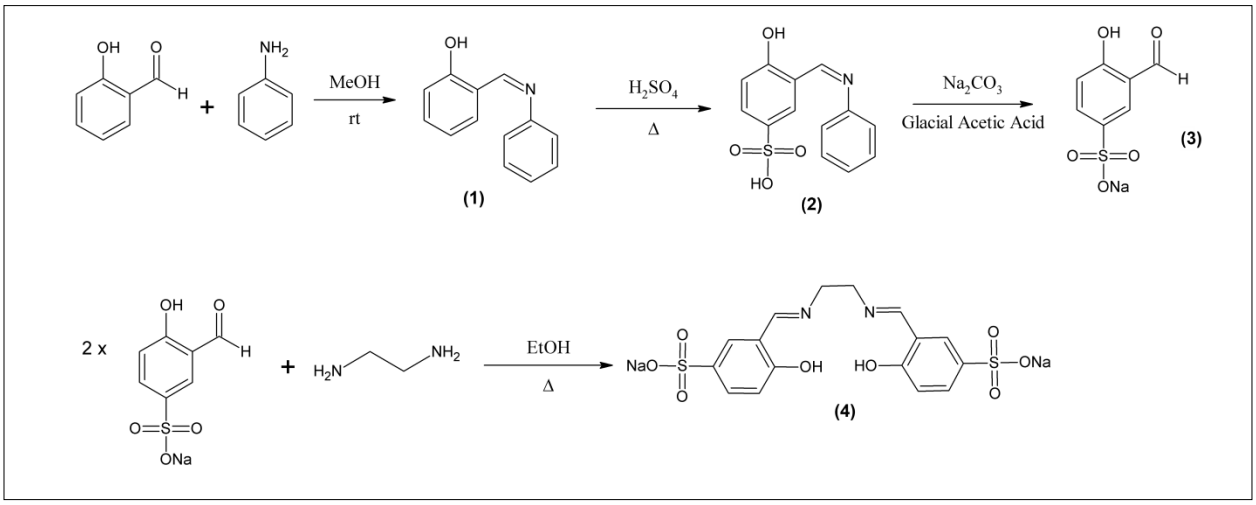

The pale yellow product (4) was collected after drying *in vacuo* (1.07 grams, 85% yield in the final step, 24 % overall yield). Electrospray ionization (ESI) mass spectrometry was carried out using a ESI LC-TOF (Micromass LCT 3) in negative ion mode with methanol solvent and operated with Waters MassLynx software (v.4.0). ESI-MS-TOF (-ve) m/z = 213.2 (M/2 –Na). ^{1}H and ^{13}C NMR spectra were recorded using a Bruker GN-500 (500 MHz, ^{1}H) spectrometer, equipped with a BBO probe. Proton chemical shifts are reported in units of ppm (δ) by the proteo solvent signal relative to external tetramethylsilane (TMS, δ = 0.00 ppm). ^{1}H NMR (500 MHz, DMSO) δ: 3.94 (s, (CH_2)$_2$), 4H); 6.80, 6.82 (d, C(6)*H*, 2H, J_o = 8.54); 7.54 – 7.56 (dd, C(6)*H*, 2H, $J_{m,o}$ = 2.16, 8.53); 7.70, 7.71 (d, C(6)*H*, 2H, J_m = 2.14); 8.69 (s, C*H*N, 2H), 13.61 (br s, C(6)O*H*, 2H). ^{13}C{^{1}H} NMR (500 MHz, DMSO) δ: 58.9 (CH_2); 116.3, 117.6, 129.4, 130.5 (*C*(6)-CH_2-N and *C*(6)-H), 139.7(Ph-SO_3), 161.5 (CH=N), 167.5 (Ph-O). The NMR spectra are provided as Figures S1 and S2.

Fig. S1. ^{1}H NMR Spectrum of H_2salen-SO_3

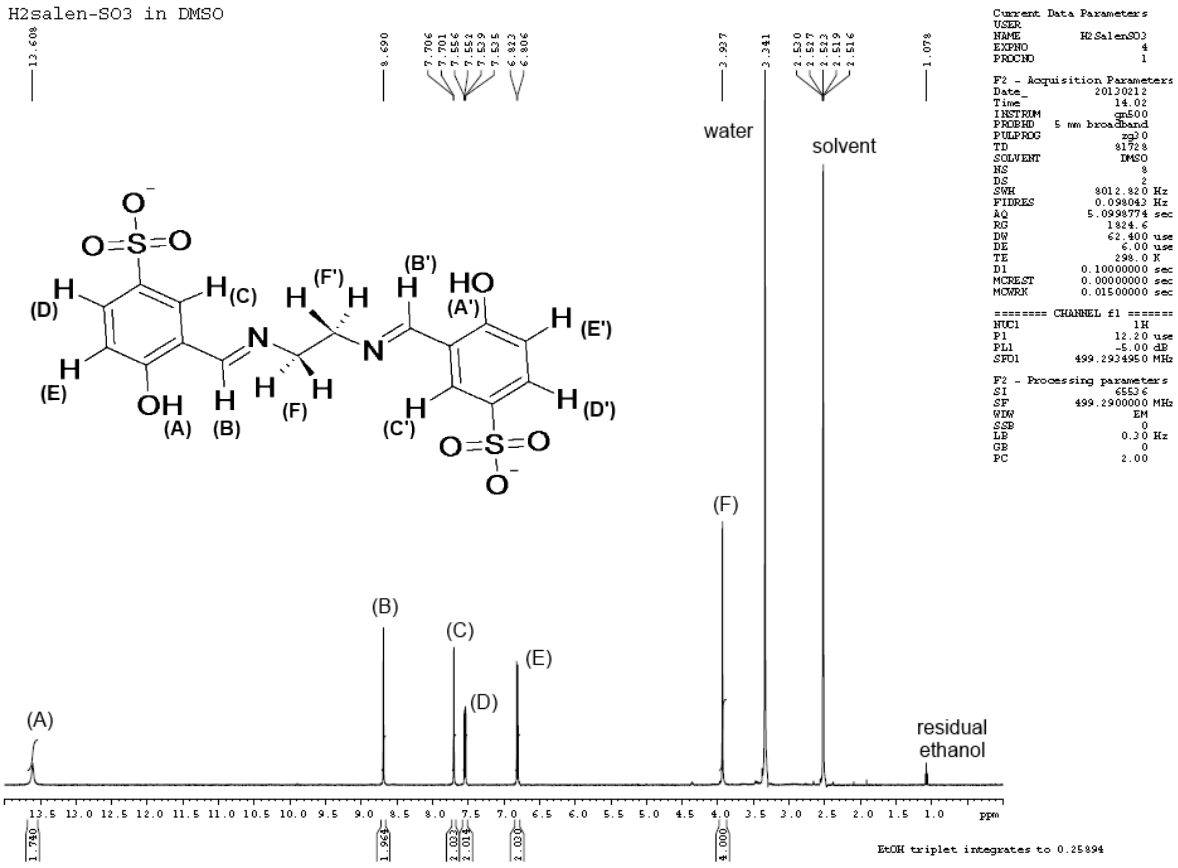

Fig. S2. $^{13}C\{^{1}H\}$ NMR Spectrum of H_2salen-SO_3

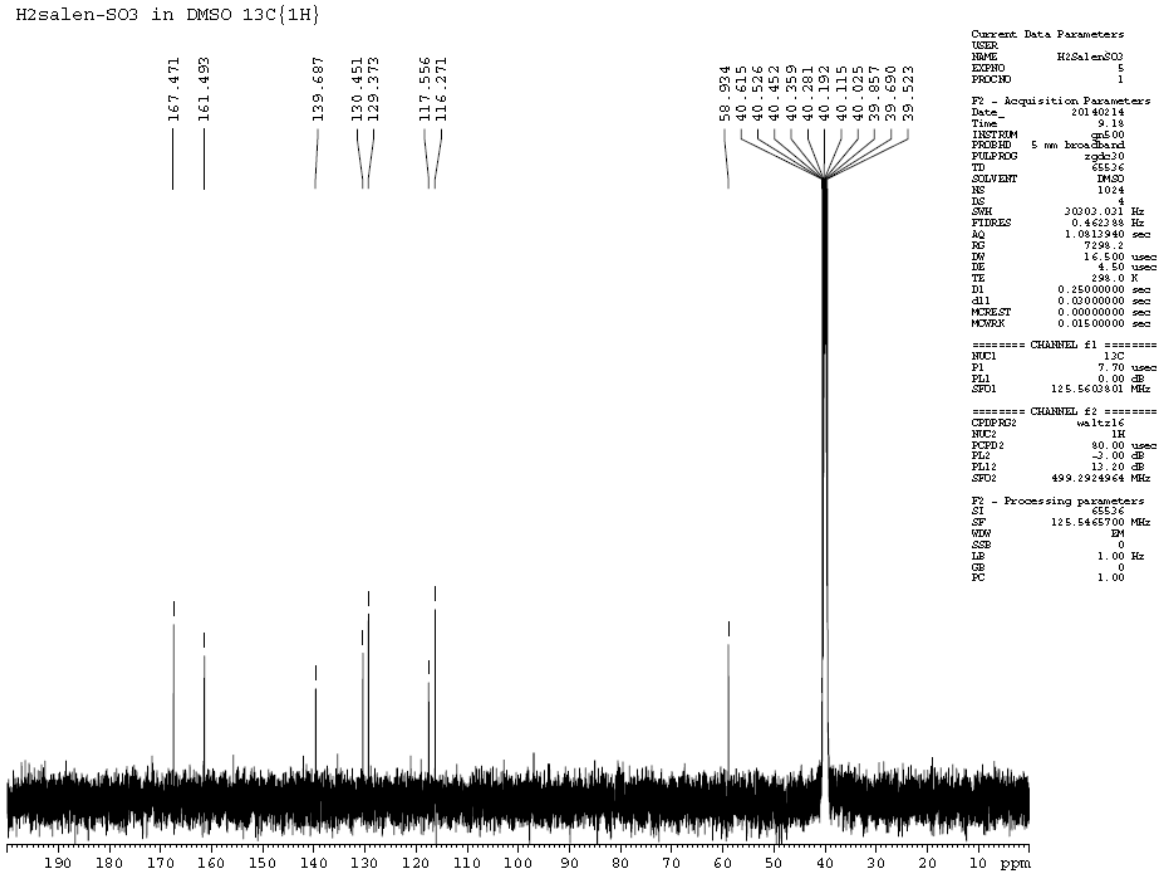

Synthesis of Disodium [*N,N'*-ethylenebis(salicylidene-5-sulfonato)iminato](aqua)dioxouranium nonahydrate.

An aqueous solution of uranyl nitrate (0.050 g U, 0.21 mmol) in H_2O (2 ml) was evaporated to dryness with heat and allowed to cool to room temperature. To the resultant uranyl nitrate hydrate yellow solid *N,N'*-bis(salicylidene-5-sulfonato)-diaminoethane disodium salt (0.099 g, 0.21 mmol) dissolved in water (1 ml) was added, with stirring, to produce an immediate intense red colored solution. The pH was recorded as 3.3, and adjusted to pH 7.7 through the drop-wise addition of 1 M NH_4OH. The solution was filtered through glass wool supported in a Pasteur pipette and allowed to evaporate yielding an orange solid that was collected, washed with ethanol and air dried (0.159 g, 74 % yield based on 9 crystallized water molecules). Crystals of $Na_2[UO_2(salen\text{-}SO_3)(OH_2]\cdot 9H_2O$ were obtained by slow evaporation of a solution as prepared above over several weeks with a starting pH of 7.6.

Structural Characterization of $Na_2[UO_2(salen\text{-}SO_3)(OH_2]\cdot 9H_2O$

Crystal data: $C_{32}H_{34}Na_{32}N_2O_5S_6U$, M = 1025.97, triclinic, a = 8.4220(11), b = 9.3646(12), c = 19.946(3) Å, α = 89.043(1), β = 88.581(1), γ = 72.240(1)°, V = 1497.6(3) $Å^3$, T = 140(1) K, space group P-1, Z = 2, D_c = 2.041 g cm^{-3}, Mo-K radiation (λ = 0.71073 Å), μ = 5.674 mm^{-1}, orange block with dimensions 0.50 x 0.30 x 0.10 mm, 16975 reflections measured, 6864 unique reflections (R_{int} = 0.0139), 6724 reflections with I> 2σ(I). Final R (I> 2σ (I)), R_1 = 0.0166, ωR_2 = 0.0170. Final R (all data), R_1 = 0.0570, ωR_2 = 0.0572.

	1	**2**	**3**	**4**	**5**
U1 – O1 (yl)	1.7898(19)	1.763(13)	1.775(5)	1.790(3)	1.769(5)
U1 – O2 (yl)	1.7703(19)	1.772(15)	1.772(5)	1.786(5)	1.764(5)
U1 - O3 (salen)	2.2740(18)	2.245(14)	2.235(5)	2.259(5)	2.277(5)
U1 - O4 (salen)	2.2829(18)	2.330(32)	2.298(5)	2.263(5)	2.286(5)
U1 – N1 (salen)	2.526(2)	2.572(24)	2.560(6)	2.586(6)	2.548(6)
U1 – N2 (salen)	2.566(2)	2.542(47)	2.571(6)	2.396(5)	2.563(6)
O1- U1 – O2	178.74(7)	178.6(0.6)	179.5(2)	178.72(2)	178.98(6)
O3 – U1 – O11	78.78(6)	77.4(0.4)	78.2(3)	77.02(18)	78.91(18)
O4 – U1 – O11	79.84(6)	78.3(0.4)	77.4(2)	80.74(17)	79.11(17)
O4 – U1 – N2	69.22(7)	68.8(0.5)	69.1(2)	69.67(18)	69.76(18)
O3 – U1 – N1	69.15(7)	70.0(0.4)	69.0(2)	61.50(19)	69.68(17)
N1 – U1 – N2	65.30(7)	66.2(0.4)	66.1(2)	66.92(19)	64.84(18)

Table S.1. Selected bond lengths (Å) and bond angles (°) for $[UO_2(salen\text{-}SO_3)(OH_2)]^{2-}$ (1), UO_2(salen)(MeOH) (2), UO_2(salen)(EtOH) (3), UO_2(salen)(TPPO) (4) and UO_2(salen)(OH_2) (5).

Fig. S3. View of part of the extended structure of $Na_2[UO_2(salen\text{-}SO_3)(OH_2]\cdot 9H_2O$, showing that only one of the two sulfonate groups in $[UO_2(salen\text{-}SO_3)(OH_2]^{2-}$ is coordinated to sodium cations.

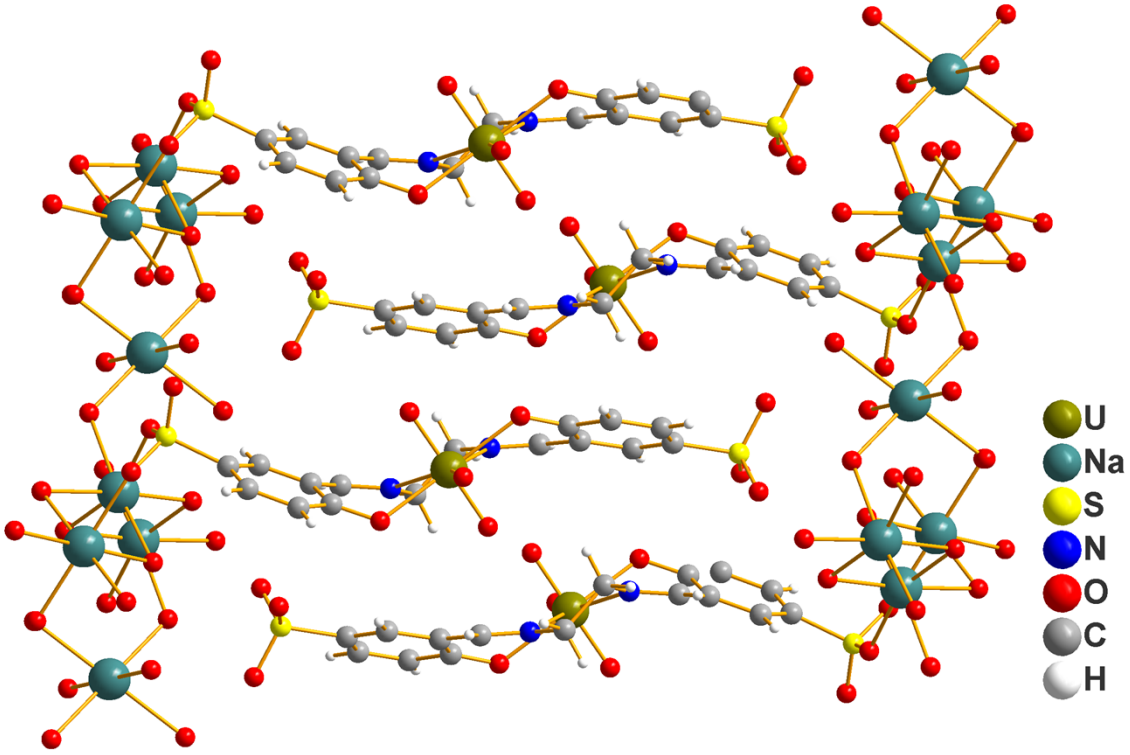

The extended structure reveals anions of $[UO_2(salen\text{-}SO_3)(OH_2)]^{2-}$ stacked in layers such that only the sulfonato oxygen atoms associated with the S1 sulfur atom coordinate to the hydrated sodium atoms linking adjacent stacked layers (O6-Na1 = 2.366 Å & O7-Na2 = 2.375 Å), with no O-Na interactions involving the sulfonato oxygen atoms relating to the S2 sulfur. The different sulfonyl group environments could be the reason for the observation of two distinct IR vibrations (Fig. S4) in the $\nu_{asym}(SO_3)$ region (1219 & 1192 cm^{-1}), and a vibration (1039 cm^{-1}) with a distinct lower energy shoulder in the $\nu_{sym}(SO_3)$ region.[5-7] The IR spectrum of $Na_2[UO_2(salen\text{-}SO_3)(OH_2)]\cdot 9H_2O$ also has characteristic C=N and C=C stretches at 1630 and 1597 cm^{-1}, respectively, which are comparable to similar assignments for uranyl salen complexes.[8-9] A series of overlapping transitions between 900-950 cm^{-1} prevented the assignment of the asymmetric uranyl stretching vibration, which was observed between 880-930 cm^{-1} for other uranyl(VI) salen complexes.[8-9] In contrast, the symmetric uranyl stretch was observed in both the IR (831 cm^{-1}) and Raman (832 cm^{-1}) spectra of $Na_2[UO_2(salen\text{-}SO_3)(OH_2)]\cdot 9H_2O$. This symmetric uranyl stretch is often only Raman active, with no change in dipole moment. However, the lowered molecular symmetry due to the step conformation of certain uranyl Schiff base complexes, as now also observed with the sulfonated salen complex discussed here, has been postulated as the reason for this vibration being IR active.[9]

Fig. S4. IR/Raman Spectra of $Na_2[UO_2(salen\text{-}SO_3)(OH_2)]\cdot 9H_2O$.

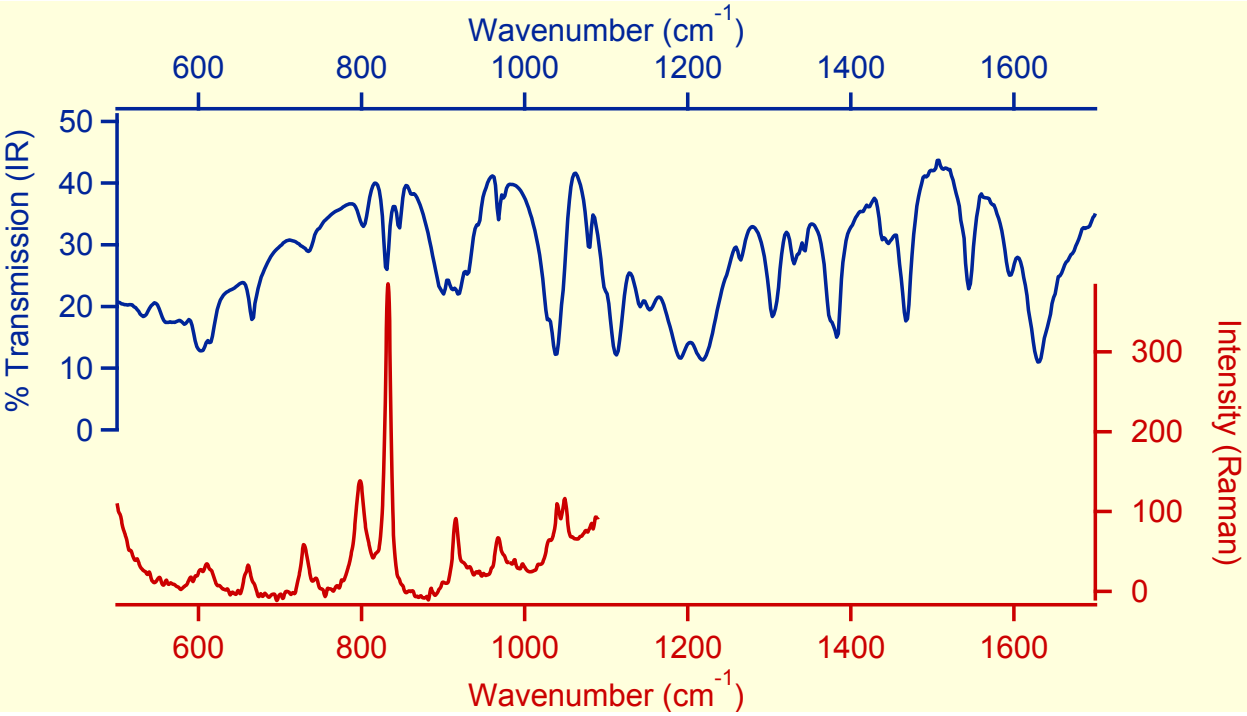

Competitive Extraction.

Extraction studies were conducted using 0.01 mol L^{-1} HDEHP in toluene as the organic phase and 0.01 mol L^{-1} H_2salen-SO_3 in 0.1 mol L^{-1} KNO_3 with 0.01 mol L^{-1} acetic acid (equilibrium pC_H = 5.3) as the aqueous phase – the aim being to investigate the partitioning behavior of U(VI) and Eu(III). Although, in previous studies solutions were prepared in ammonium acetate buffer to mitigate pH excursions, this buffer proved to be intractable in liquid-liquid extraction, because the equilibrated phases left a thick white emulsion at the interface. Instead, acetic acid was used to adjust the acidity of the initial aqueous solution and proved to be useful in avoiding drastic changes in acidity post-extraction. The aqueous phase was prepared by dissolving 0.0236 g of the H_2salen-SO_3 sodium salt (5.00 x 10^{-5} mol) in 0.1 mol L^{-1} KNO_3 (pC_H 4.4) containing 1 x 10^{-4} mol L^{-1} $UO_2(NO_3)_2$ - adjusting the pC_H back down to 5.3 using 0.2 cm^{-3} of 0.2 mol L^{-1} acetic acid. The experiments employed continuous contact between 5 cm^{-3} of the organic phase pre-equilibrated with the aqueous phase without metal ion present and 5 mL the aqueous phase containing the metal ions (U and Eu). The time-dependent partitioning of $\{UO_2\}^{2+}$ (1 x 10^{-4} mol L^{-1}) and Eu^{3+} (1 x 10^{-5} mol L^{-1} radiotracer + carrier) in the presence of $\{UO_2\}^{2+}$ (1 x 10^{-4} mol L^{-1}) were examined in two separate experiments by rapid stirring with a magnetic stir bar to generate an emulsion. The concentration of $\{UO_2\}^{2+}$ was chosen to provide sufficient count rates after neutron activation of the samples. The specific activity of the lanthanide radiotracer was high enough to maintain a concentration of 1 x 10^{-5} mol L^{-1} Eu(III) and 3 x 10^{-4} mol L^{-1} for all metal ions in order to avoid exceeding the metal cation capacity of the organic phase and mitigate the formation of polymeric species. At each timepoint, the phases were disengaged by centrifugation and equal volume aliquots of the phases were removed and sampled in triplicates of 100 µL for analysis. Comparison to extraction without the holdback reagent was made possible by preparing a similar system without H_2SalenSO_3 present and contacting for 30 min. The extent of extraction was calculated as a distribution ratio (ratio of summed gamma count rates in equilibrated organic phase to that in the aqueous phase).

The $^{152/154}$Eu tracer was prepared by irradiating a sample of Eu_2O_3 in the UC Irvine Mark I TRIGA reactor (estimated thermal neutron flux of 5 x 10^{12} n*$cm^{-2*}s^{-1}$, 10 hours) followed by dissolution of the oxide in nitric acid as described previously. Uranium samples were transferred to 1.4 mL neutron activation analysis (NAA) polytubes (LA Container, Yorba Linda, CA) containing a small piece of Kim wipe for sorbing the liquid at the base of the cylindrical tube before heat sealing the lids. An 8 mL NAA polytube was used for secondary containing and was heat sealed as well. These samples were irradiated in the rotary specimen rack “lazy susan” of the UC Irvine Mark I TRIGA nuclear reactor for 1 hour at 250 kW

(estimated neutron flux of 8 x 10^{11} n cm^{-2} s^{-1}). The secondary 8 mL tubes were rinsed with water, cut, and removed. The ^{239}U ($t_{1/2}$ = 23.45 minutes) was allowed to decay, whereupon the primary 1.4 mL tubes were enclosed in plastic sandwich bags for counting of ^{239}Np ($t_{1/2}$ = 2.36 days) decay gamma rays (spectral region: 95.9– 110.1 keV; values in order of E_γ (keV), γ(%), mode: 99.52, 15.0, Pu $K_{\alpha 2}$; 103.73, 23.9, Pu $K_{\alpha 1}$; 106.13, 22.7, γE1 + 0.3%M2).[10] ^{239}Np gamma counting was undertaken using a Canberra high purity germanium (HPGe) detector with a 30% relative efficiency operated with Genie^{TM} 2000 (v. 3.2.1) gamma acquisition and analysis software. Prior to positioning each sample over the HPGe, the inserted Kim wipe was forced to the base to ensure consistent geometry. Count rates were normalized to the reactor scram time (end of sample irradiation) and counting errors were calculated by the software. Europium samples were analyzed in gamma counting polytubes by a Packard Cobra 5003 automatic gamma counter. Overall uncertainties in the measurements were reported as the sum of the relative counting errors relative standard deviations from triplicate samples at the 95% confidence interval. Mass balance recoveries (all between 94% and 111%) were determined by the ratio of the sum of count rates in both phases post-phase contact to the count rate for the metal ion-spiked aqueous solution used in the extraction.

^{1}H NMR Spectra for H_2salen-SO_3 in Aqueous Solution with $\{UO_2\}^{2+}$

The intents of these experiments were to observe the effect of $\{UO_2\}^{2+}$ on the proton spectrum of the ligand and characterize the dominant complex(es) in solutions under conditions close to those of the competitive extraction. Samples were prepared by dissolving a known weight of the solid H_2salen-SO_3 sodium salt in varying concentrations (0 mol*L^{-1} to 2.00 x 10^{-2} mol*L^{-1}) of $UO_2(NO_3)_2$ in solution with 0.1 M KNO_3 at pC_H 4 (adjusted using acetic acid). Each $UO_2(NO_3)_2$ concentration was prepared as a separate solution for analysis. The weight of the ligand and the total volume were held constant such that the formal concentration of the ligand was 1.0 x 10^{-2} mol*L^{-1}. To a 0.750 cm^{-3} portion of these solutions, 0.250 cm^{-3} of D_2O (99.98%, Cambridge Isotope Labs, Tewksbury, MA, USA) was added and the solutions were allowed to equilibrate for at least one hour prior to acquiring the spectra. Proton NMR spectra were recorded using a Bruker GN-500 (500 MHz, ^{1}H) spectrometer, equipped with a BBO probe and employing gradient pulses for water solvent suppression.[11] Due to the prevalence of water in these samples, the phenolic protons are not observable. Thus, the spectral width was maintained at 16 ppm centered at 4.9 ppm.

Fig. S5. ^{1}H NMR Spectra (Downfield) of H_2salen-SO_3 with and without U(VI) in Aqueous Solution

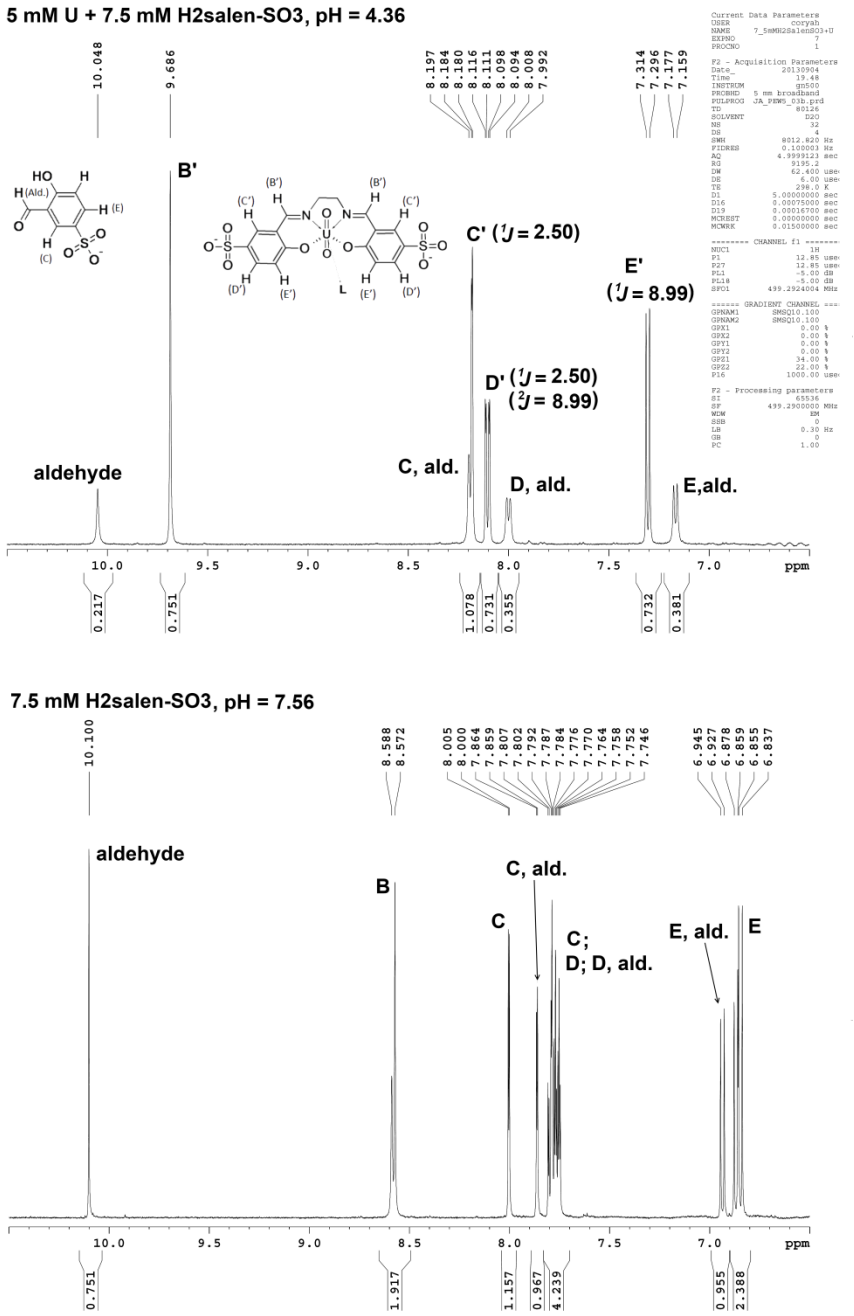

Figure S5 contains the downfield portion (6.5 ppm to 10.5 ppm) of the ^{1}H NMR spectra of the pre-addition (bottom trace) and post-equivalence (top trace) solutions in the titration of 7.5 x 10^{-3} mol*L^{-1} (formal concentration) H_2salen-SO_3 by $UO_2(NO_3)_2$. The peak label convention is the same as in Figure S1, with both the intact ligand and 5-sulfonato-salicylaldehyde phenyl proton resonances collectively labeled C, D and E. Signals of salen-SO_3 that have shifted due to complexation are labeled with a prime (') symbol. Integrals have been calibrated to the ethylenediamine singlet shown in Fig. S6. The ligand signals are best identified by the doublet-of-doublets at 6.8 ppm (E), the doublet (C) at 8.0 ppm, and the azomethine singlets at 8.6 ppm, as they shift in the presence of $\{UO_2\}^{2+}$ to 7.3 ppm, 8.2 ppm and 9.6 ppm, respectively. For two reasons, the spectrum for the ligand alone (bottom trace) is more complex than that in DMSO (Fig. S1). Firstly, there is presence of the 5-sulfonato-salicylaldehyde resonance (δ 10.1 ppm), while the azomethine (B) signal remains, indicating that partial hydrolysis occurred in aqueous solution. Secondly, the average states are due to tautomerization or partial hydrolysis of the intact ligand under these conditions, resulting in two significantly different environments of the phenyl protons (C, D, E), as well as the azomethine proton (B).

Complexation with $\{UO_2\}^{2+}$ is apparent by the shift of the azomethine signal downfield by more than 1 ppm as a singlet. In fact, all of the salen-SO_3 resonances in this region shift downfield due to deshielding of these nuclei upon LMCT. As a consequence of the spin-orbit contributions to the electronic structure of the $\{UO_2\}^{2+}$ unit, a weak paramagnetic field has been demonstrated to affect the observed shifts of susceptible nuclei proximal to and in the region perpendicular to the cation axis.[12] These electric field effects may also coincide with electronic effects from the coordination of U(VI) with the π-conjugated system. However, because the pH changes during the course of the titration coincide with the estimated phenolic acid dissociation constants ($pK_{a,1}$ = 4.6 and $pK_{a,2}$ = 8.9), the largest contributions to line broadening are likely from chemical exchange between tautomeric states and partial hydrolysis products. When the metal ion concentration exceeds equivalence ($\{UO_2\}^{2+}$ > 4.3 x 10^{-3} mol*L^{-1}, spectrum not shown), the signals of the complex are sharp. In contrast, the resonances of the aldehyde hydrolysis product are broad, suggesting weak interaction of the metal ion with the aldehyde or, in general, chemical exchange. Further verification of these assignments is found in the increasing symmetry of the aromatic region at 5 x 10^{-3} mol*L^{-1} $\{UO_2\}^{2+}$, where six dominant proton environments account for the six mutually degenerate Ph-H resonances of salen-SO_3 and three Ph-H signals from the aldehyde. Interestingly, the mole fraction percent of aldehyde with respect to the sum of the integrals (aldehyde) and (B') diminishes from 44% for the ligand alone to 36% at 5 mM U(VI). Because the diminished

aldehyde response is also seen in similar solutions of 5-sulfonato-salicylaldehyde alone, it may be due to formation of the *gem*-diol (hydrate) in aqueous solution.

Fig. S6. ^{1}H NMR Spectra (Upfield) of H_2salen-SO_3 with and without U(VI) in Aqueous Solution

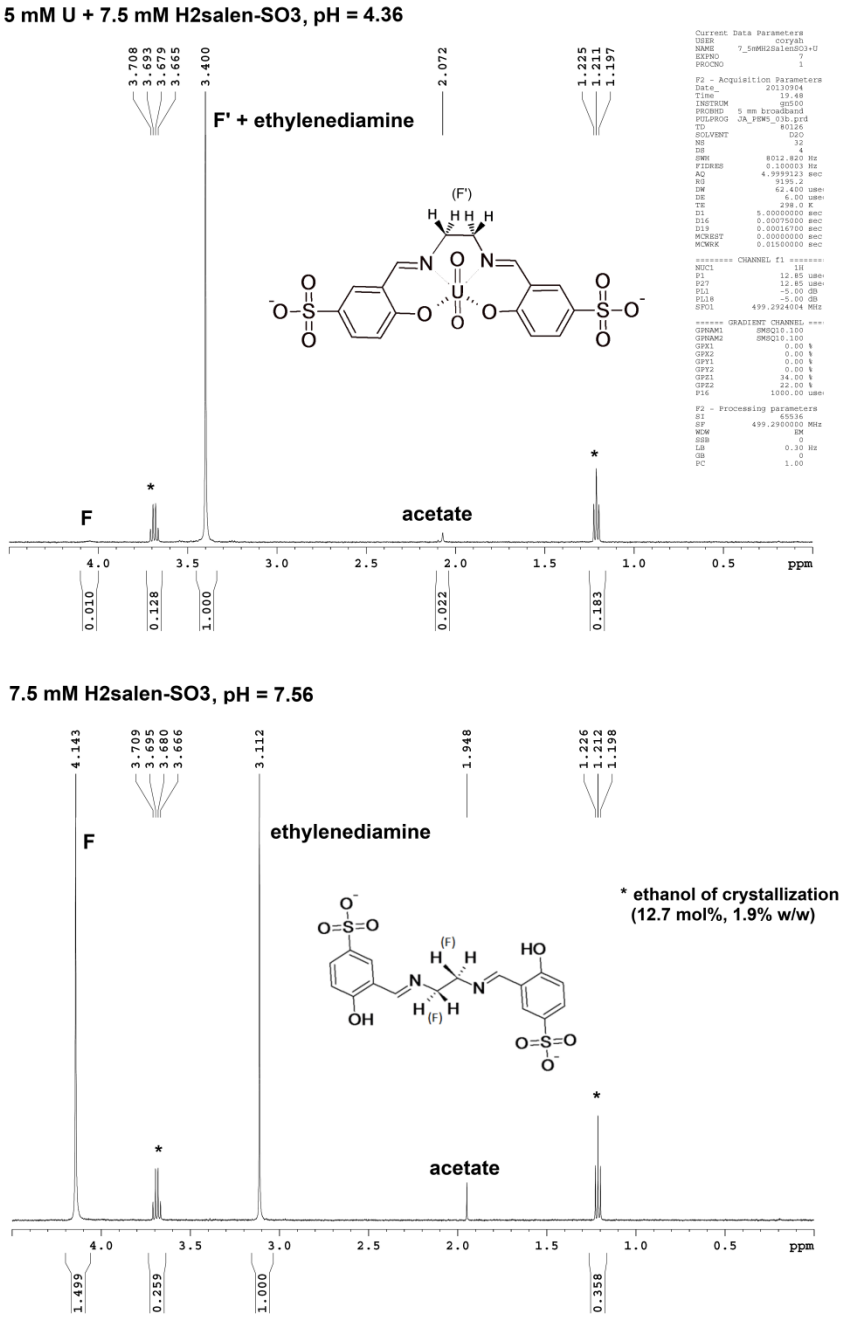

In the aliphatic region of these spectra, presented in Figure S6, the ethylenediimine singlet (F, δ 4.1 ppm) of the intact ligand (bottom trace) is distinguished from the ethylenediamine singlet (δ 3.1 ppm) resulting from ligand hydrolysis. At the same time that the ligand singlet (F) shifts upfield by 0.1 ppm and nearly vanishes after exceeding an equivalence of $\{UO_2\}^{2+}$, the ethylenediamine peak shifts downfield by 0.3 ppm as a sharp singlet. These shifts may be attributed to the change in pH from cation exchange of the phenolic protons with uranyl and the lower pH of the uranyl nitrate titrant. Likewise, a two-fold increase in the intensity of the ethylenediamine singlet (employing the ethanol signals as internal standard) and its shift downfield suggest that further hydrolysis occurs as the pH decreases, an effect that is reflected by the 2-fold decrease of Ph-H (C, D and E to C', D'and E') and azomethine (B to B') integrals in Fig. S5. On the other hand, because an effective 2-fold loss in the combined B, C, D and E resonances (Fig. S5) and the ethanol triplet (1.2 ppm) can be attributed to calibration of these integrals to the 2-fold increased ethylenediamine signal, the salicylidene units can be reasonably assumed to remain intact at the end of the titration. Doubling of the ethylenediamine signal is, therefore, consistent with ethylene protons F' experiencing the same field strength as those of the ethylene hydrolysis product. A paramagnetic field effect cannot be ruled-out in the line broadening of the ethylene resonance of the complex (F'), especially because these protons would be likely closest to and within a short angle of the uranyl center. However, electronic and paramagnetic field effects may be difficult to distinguish.[12] Taken together with the well-resolved downfield signals of the Ph-H protons and a sharp azomethine singlet of the complex (B', top trace) these results indicate that that the rings are in rather symmetrical environments and that the complex is formed with the intact ligand. Thus, a single UO_2(salen-SO_3) complex is expected to exist under conditions similar to those in the extraction (Figure 3).

It is important to point out that changes in pH are inevitable for an ion-exchange reaction outside of well-buffered solutions. A higher initial pH can be ascribed to the hydrolytic production of the base (pK_a = 9.9) ethylenediamine upon dissolution. Then, addition of the lower pH uranyl nitrate solution and the subsequent cation exchange reaction increase both the hydrogen ion concentration. Also noteworthy, the methyl singlet of acetate shifts, broadens and splits after equivalence due to complexation with the uranyl ion, somewhat like the aldehyde resonances, which is consistent with the higher order stability of the UO_2(salen-SO_3) complex. Experiments to test whether the broad and split peaks of the ligand are due primarily to chemical exchange or paramagnetic field/electronic effects are currently underway.

References.

1. J.A. Partridge, R.C. Jensen, *J. Inorg. Nucl. Chem.*, 1969, **31**, 2587.
2. K.J. Berry, F. Moya, K.S. Murray, A.B. van den Bergen, and B.0. West, *J. Chem. Soc., Dalton Trans.*, 1982, 109.
3. M. Botsivali, D. F. Evans, P. H. Missen, and M. W. Upton, *J. Chem Soc., Dalton Trans.*, 1985, 1147.
4. D. F. Evans and P. H. Missen, *J. Chem. Soc., Dalton Trans*., 1985, 1451.
5. C. Bauer, P. Jacques and A. Kalt., *Chem. Phys. Lett*., 1999, **307**, 397.
6. E. Delahaye, S. Eyele-Mezui, J.-F. Bardeau, C. Leuvrey, L. Mager, P. Rabu and G. Rogez, *J. Mater. Chem.,* 2009, **19**, 6106.
7. E. Delahaye, M. Diop, R. Welter, M. Boero, C. Massobrio, P. Rabu and G. Rogez, *Eur. J. Inorg. Chem.* 2010, 4450.
8. L. Cattalini, S. Degetto, M. Vidali and P. A. Vigato, *Inorg. Chim. Acta*, 1971, **6**, 173.
9. H. C. Hardwick, D. S. Royal, M. Helliwell, S. J. A. Pope, L. Ashton, R. Goodacre and C. A. Sharrad, *Dalton Trans*., 2011, **40**, 5939.
10. E. Browne, R.B. Firestone in *Table of Radioactive Isotopes*, Wiley-Interscience, New York, USA, 1986, p. 329-2.
11. T.-S. Hwang, A.J. Shaka, *J. Mag. Reson. A*, 1995, **112**, 275.
12. a) J.C. Eisenstein, M.L.H. Pryce, *Proc. R. Soc. Lond. A*, 1955 229. b) T.A. Sidall III, C.A. Prohaska, *Inorg. Chem.*, 1965, **4**, 783. c) T. F. Wall, S. Jan, M. Autillo, K.L. Nash, L. Guerin, C. Le Naour, P. Moisy, C. Berthon, *Inorg. Chem.* 2014, **53**, 2450.